Breakup of nanoparticle clusters using microfluidizerM110-P

BREAKUP OF NANOPARTICLE CLUSTERS USING MICROFLUIDIZER M110-P

Emmanuela Gavi [(1)], Dominik Kubicki [(2)], Gustavo A. Padron[(3)], N. Gül Özcan-Taşkın [(4)]

(1) Now at F. Hoffmann- La Roche, Basel, Switzerland

(2) Now at Engineering Design Center Al. Krakowska 110/114 02-256 Warsaw, Poland

(3) BHR Group, Cranfield, Bedfordshire MK43 0AJ UK

(4)Author to whom correspondence should be sent: N.Ozcan-Taskin@lboro.ac.uk

Loughborough University, Dept. of Chemical Engineering, Loughborough LE11 3TU, UK

Abstract A commercial design, bench scale microfluidic processor, Microfluidics M110-P, was used to study the deagglomeration of clusters of nanosized silica particles. Breakup kinetics, mechanisms and the smallest attainable size were determined over a range of particle concentrations of up to 17% wt. in water and liquid viscosities of up to 0.09 Pa s at 1% wt. particle concentration. The device was found to be effective in achieving complete breakup of agglomerates into submicron size aggregates of around 150 nm over the range covered. A single pass was sufficient to achieve this at a low particle concentration and liquid viscosity. As the particle concentration or continuous phase viscosity was increased, either a higher number of passes or a higher power input (for the same number of passes) was required to obtain a dispersion with a size distribution in the submicron range.

Breakup took place through erosion resulting in a dispersion of a given mean diameter range regardless of the operating condition. This is in line with results obtained using rotor-stators. Breakup kinetics compared on the basis of energy density indicated that whilst Microfluidizer M110-P and an in-line rotor-stator equipped with the emulsor screen are of similar performance at a viscosity of 0.01 Pa s, fines volume fraction achieved with the Microfluidizer was much higher at a viscosity of 0.09 Pa s.

Keywords: Microfluidizer M110-P, dispersion of nanoparticles, breakup, fragmentation, deagglomeration

1. INTRODUCTION

Microfluidic processors are employed for power intensive processes such as size reduction in emulsions (Lee and Norton, 2013; Persson et al, 2014; Bai and McClements, 2016), solid-liquid dispersions (Yurdakul et al, 2012), liposomes (Lajunen et al, 2014), cell rupture (Choi et al, 1997; Stupak et al, 2015) or as reactors for the synthesis of nanomaterials (Chomistek and Panagiotou, 2009; Panagiotou et al, 2009). These processes are common to a wide range of industries from pharmaceuticals, nutraceuticals, inks, coatings and bioindustries.

This study was performed with a commercial design microfluidic processor to assess its performance in deagglomerating clusters of nanosize silica particles. The last two decades have seen rapid uptake of nanotechnology with the development of new products of improved performance or formulations with properties that are not possible to achieve otherwise. The development of new formulations brings the requirement of process design and scale up to enable the market introduction of these novel products. Large scale manufacture of nanoparticles is more commonly achieved through flame pyrolysis with the resulting powder consisting of agglomerates and aggregates of primary particles. A key step during the manufacture of an intermediate or final product in the form of a liquid based nanoparticle dispersion is the deagglomeration of these clusters of nanoparticles to achieve a fine dispersion. Deagglomeration can occur through erosion, rupture or shattering as shown in Figure 1.a, resulting in different evolutions of the Particle Size Distribution (PSD) during the course of processing as shown in Figure 1.b (Özcan-Taşkın et al., 2009).

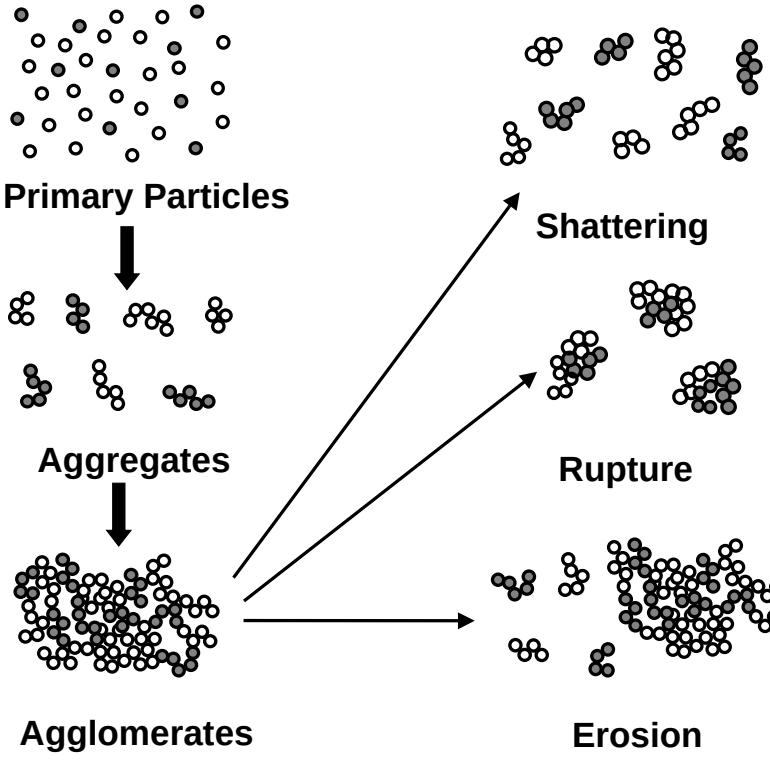

Figure 1.a Mechanisms of breakup of nanoparticle clusters

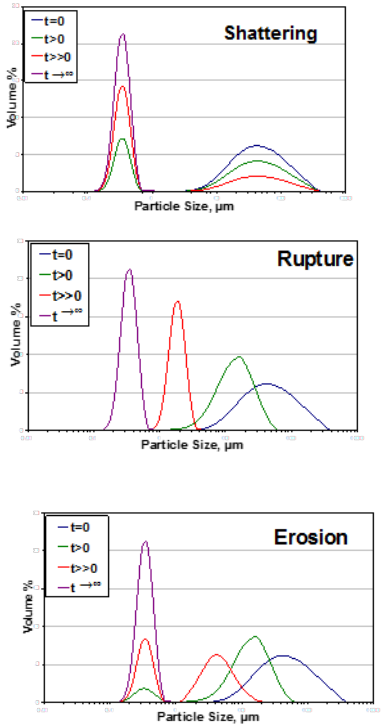

Figure 1.b Evolution of the PSD for different breakup mechanisms (Özcan-Taşkın et al., 2009)

Commonly used impellers, such as turbines and hydrofoils, do not provide sufficiently high levels of power input to achieve deagglomeration into the sub-micron range (Xie, et al, 2007). Therefore, power intensive process devices such as sawtooth impellers (Xie et al, 2007), batch (Xie et al, 2007; Kamaly et al, 2017) or in-line rotor-stators (Baldyga et al, 2008; Padron et al, 2008; Özcan-Taşkın et al., 2016), high pressure jets (Wengeler et al, 2006; Sauter and Schuchmann, 2007) are employed. The hydrodynamic stresses in the flow field generated in such devices are sufficiently high to overcome the tensile strength of the agglomerates in order for breakup to occur. In the laminar regime, shear and/or extensional stresses (τ, Pa) cause breakup:

$$\tau = \mu \dot{\gamma} \quad [1]$$

where μ (Pa s) the shear or extensional viscosity and $\dot{\gamma}$ (s) is either the shear or extensional rate. In the turbulent regime, breakup occurs as a result of turbulent stresses acting on agglomerates. Agglomerates may be of a size L_i such that $l \gg L_i \gg \lambda_k$, l being macroscale of turbulence and λ_k, Kolmogorov microscale:

$$\lambda_k = \frac{\nu^{3/4}}{\varepsilon^{1/4}} \quad [2]$$

where ν (m^2 s^{-1}) is the kinematic viscosity and ε (m^2 s^{-3}) the local energy dissipation rate per unit mass of liquid for which the frequency of turbulence (f) is defined as follows:

$$f = \frac{\varepsilon^{1/3}}{L_i^{2/3}} \quad [3]$$

These will be broken up through eddies in the inertial subrange of turbulence,

$$\tau \propto \rho \varepsilon^{2/3} L_i^{2/3} \quad [4]$$

where ρ (kg m^{-3}) is density. Agglomerates of a size $L_i < \lambda_k$ are broken up through viscous subrange eddies (Baldyga and Bourne,1994):

$$\tau \propto \mu \left(\frac{\varepsilon}{\nu}\right)^{1/2} = \rho \nu^{1/2} \varepsilon^{1/2} \quad [5]$$

where ν (m^2 s^{-1}) is the kinematic viscosity. The frequency of turbulence in this range is given by:

$$f = \left[\frac{\varepsilon}{\nu}\right]^{1/2} \quad [6]$$

The objective of this study has been to establish the mechanism and kinetics of breakup, the smallest attainable size and the combined effects of power input (operating pressure), particle concentration and liquid phase viscosity on these. The study also included a brief comparison with an in-line rotor-stator.

2. EXPERIMENTAL

2.1 Equipment

In this study a commercial design bench top processor, Microfluidizer M110-P, from Microfluidics Corp. (Newton, MA, USA) was used. This has an open, stainless steel reservoir, in which the pre-dispersion is introduced, a reciprocating high-pressure pump, a diamond interaction chamber and a plunger in zirconia. The feed reservoir volume is 0.4 l and this was charged with 0.3 l of pre-dispersion. During operation, the pre-dispersion contained in the reservoir is forced by the high-pressure pump through the interaction chamber, experiencing very high velocities which are typically several hundred metres per second, thereby exposing the dispersion to intense impact and shear forces (Kühler et al, 2006). The detailed geometry of the interaction chamber is kept confidential, but the concept that lies behind is that the microchannel either changes direction (Z chamber) or is split and united again downstream (Y chamber) to generate high levels of stresses. A Z-type interaction chamber was used in this study, which is recommended for solid-liquid applications. Different channel sizes can be chosen depending on the application and product. The specific type used, H10Z, has a channel

size of 100 μm. The channel size of the auxiliary chamber used before the interaction chamber is 200 μm.

Some comparisons were also made with results obtained using a Silverson in-line rotor-stator, equipped with the emulsor head, EMSC, which was used in the circulation loop of stirred tank containing 100 l of dispersion (Padron and Özcan-Taşkın, 2017).

2.2 Operating procedure and conditions

The operating pressures chosen were 5, 10 and 15 kpsi which correspond to 35, 69 and 103 MPa. The manufacturers state that the pressure is maintained constant during a pulse which could be verified from the pressure gauge.

Pre-dispersions were first prepared by manually incorporating the powder in distilled water. These were subsequently sonicated for a short duration for initial size reduction to prevent the channels of the auxiliary chamber being blocked. The ultrasonicator used for the purpose was a Hielscher UP200S with the sonotrode S14D, placed in a stirred tank which was also equipped with a pitched blade turbine to ensure dispersion homogeneity. The ultrasonicator was operated at 50% amplitude for around 5- 15 min depending on the particle concentration to reach a particle size range below 200 μm before introducing the pre-dispersion into the feed chamber. Data referred to as “pass 0" in the following Section are for this sonicated pre-dispersion. The Microfluidizer was then operated at a given pressure value and the collected product was sized. If the results indicated the presence of coarse material, the dispersion was introduced back into the feed tank for another pass.

As the Microfluidizer used was not equipped with a heat exchanger, the final product temperatures were noted to be high, in some cases 60°C above room temperature.

2.2 Materials

Silica particles, Aerosil® 200V from Evonik Industries, were used as the dispersed phase. This is a native, unmodified, densified, fumed silica and the silanol groups render the silica hydrophilic. Aerosil® 200V has uses as a rheology modifier, anti-settling or anti-sagging agent in a number of products such as paints, inks, coatings, adhesives, sealants. The primary particle size is given as 12 nm, BET surface area in the range of 175- 225 m^2/g and tamped density of approximately 120 g/l by the manufacturers.

The continuous phase was either distilled water (0.001 Pa s) or glycerol solutions of 0.01 or 0.09 Pa s. At a higher viscosity of 0.73 Pa s, practical difficulties were encountered due to the entrainment of bubbles in the dispersion. This may have occurred during ultrasonication, introduction into the feed reservoir or while processing in the Microfluidizer. As the resulting dispersions contained very fine air bubbles, it was not possible to obtain reliable particle size results.

The effect of increasing the particle concentration was studied at concentrations of 1, 5, 10, 15, 17% wt. in water. Experiments on the effect of continuous phase viscosity were performed at a concentration of 1% wt. Aerosil® 200V in glycerol solutions.

2.3 Particle sizing

Particle sizes were obtained using a Beckman Coulter LS230 laser diffraction particle size analyser. This instrument combines laser diffraction and Polarization Intensity Differential Scanning (PIDS) techniques to measure particles between 0.04 – 2000 μm.

A complex refractive index of 1.46 + 0.1i was used for the dispersed phase.

2.4 Morphology

The morphology of selected samples was studied using FEI XL30 SFEG (Schottky Field-Emission Gun) analytical Scanning Electron Microscope with ultra-high resolution (UHR) lens and detector.

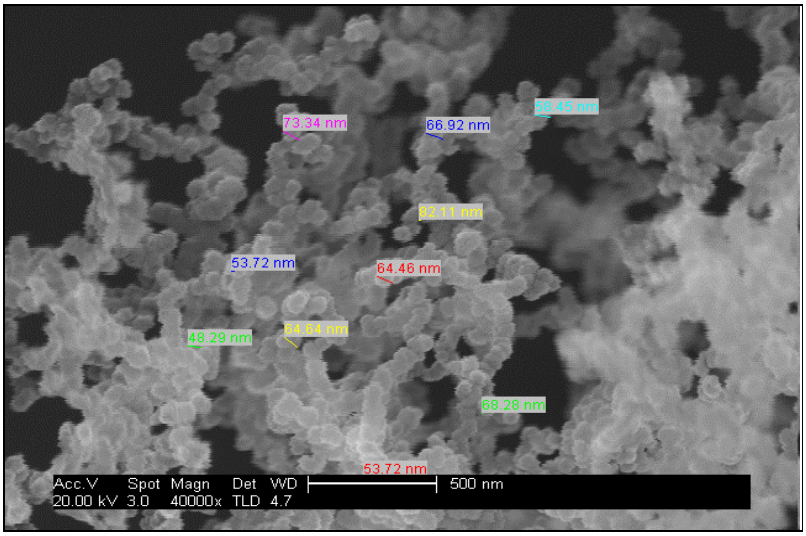

Figure 2. Morphology of Aerosil® 200V dispersions

As shown in Figure 2, the smallest structures detected were much bigger than the primary particle size of 12 nm. This would be due to the manufacturing method employed, flame pyrolysis, resulting in aggregates of fused primary particles.

2.5 Rheology

An Anton Paar Rheolab QC (Anton Paar, Hertford, UK) rheometer was used to determine the dispersion rheology. The measuring system used was the CC39 narrow gap coaxial cylinder geometry based on the German standard DIN 53019 (ISO 3219).

3. RESULTS AND DISCUSSIONS

3.1 Power input

Power input is calculated for an impulse volume (the volume of a single stroke of the reciprocating pump- V_i, m^3) as follows:

$$P = \frac{V_i}{t_i} p_i \qquad [7]$$

where P is power (W), t_i the time of impulse (s) which was quite short (typically a few seconds) and p_i, the operating pressure (Pa).

The overall flow rate was determined to be around 1.50-1.60 ml/s and the power input values are shown in Figure 3 for different continuous phase viscosities.

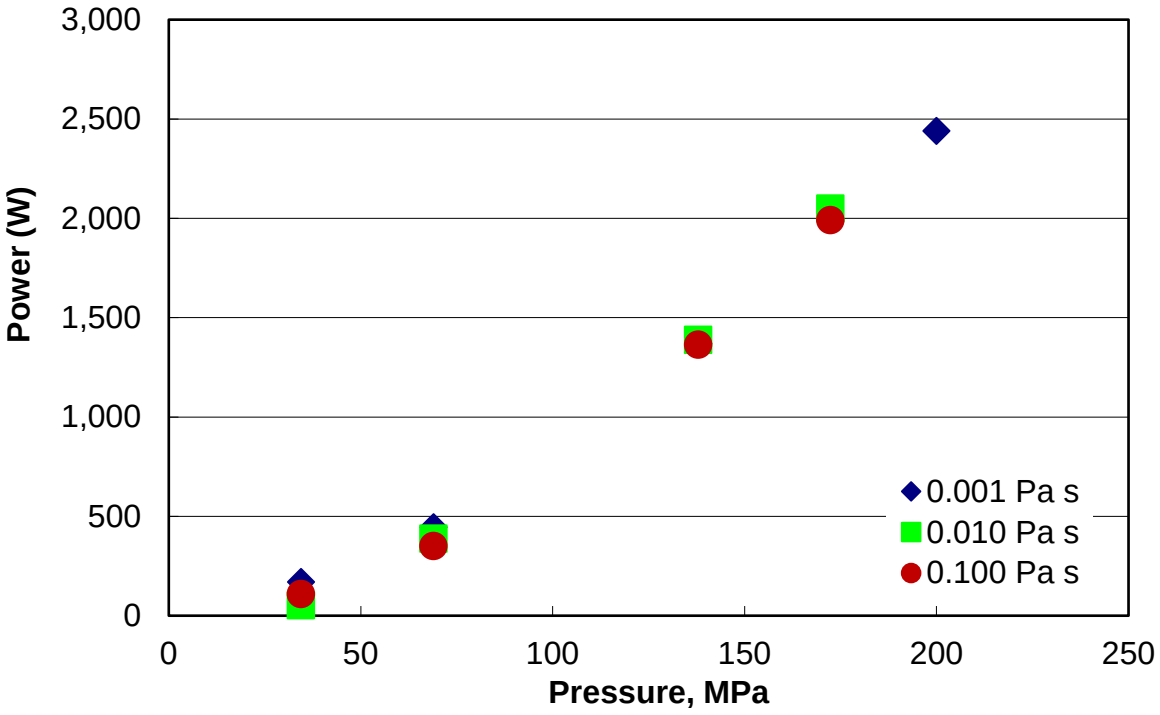

Figure 3. Power input at different operating pressures

For operating pressures of 35 to 103 MPa, covered in this study, the range of specific power input, calculated on the basis of impulse volume was 7.8×10^{3} to 1.5×10^{5} kW m^{-3}. As shown in Table 1, this is orders of magnitude higher than the range typically covered with in-line or batch rotor-stators.

Table 1. Comparison of power and specific power input by Microfluidizer M110-P with those obtained using in-line (Özcan-Taşkın et al, 2011) and batch rotor stators (Padron, 2001; Kamaly et al, 2017)

Process device	P (W)	Volume (m^3)	P/m (kW/m^3)
In-line rotor-stator	60- 1600	0.10	0.6- 16
Batch rotor-stator	0.2- 400	$(0.8- 2.5)\times 10^{-3}$	0.1- 200
Microfluidizer	45 - 850	$\sim6\times 10^{-6}$	7.8×10^{3} - 1.5×10^{5}

3.2 Dispersion rheology

The addition of 1% Aerosil® 200V in glycerol solutions did not result in a notable change in the rheological behaviour, hence glycerol based dispersions were of Newtonian behaviour with a viscosity of 0.01 and 0.09 Pa s, as shown in Figure 4. The viscosity range covered corresponds to a wide range of Reynolds numbers. Re value calculated based on the interaction chamber diameter is 3.8×10^{4} for 1% Aerosil® 200V-in-water which decreases to 7.9×10^{3} and 8.8×10^{2} in glycerol based dispersions of 0.01 and 0.09 Pa s respectively.

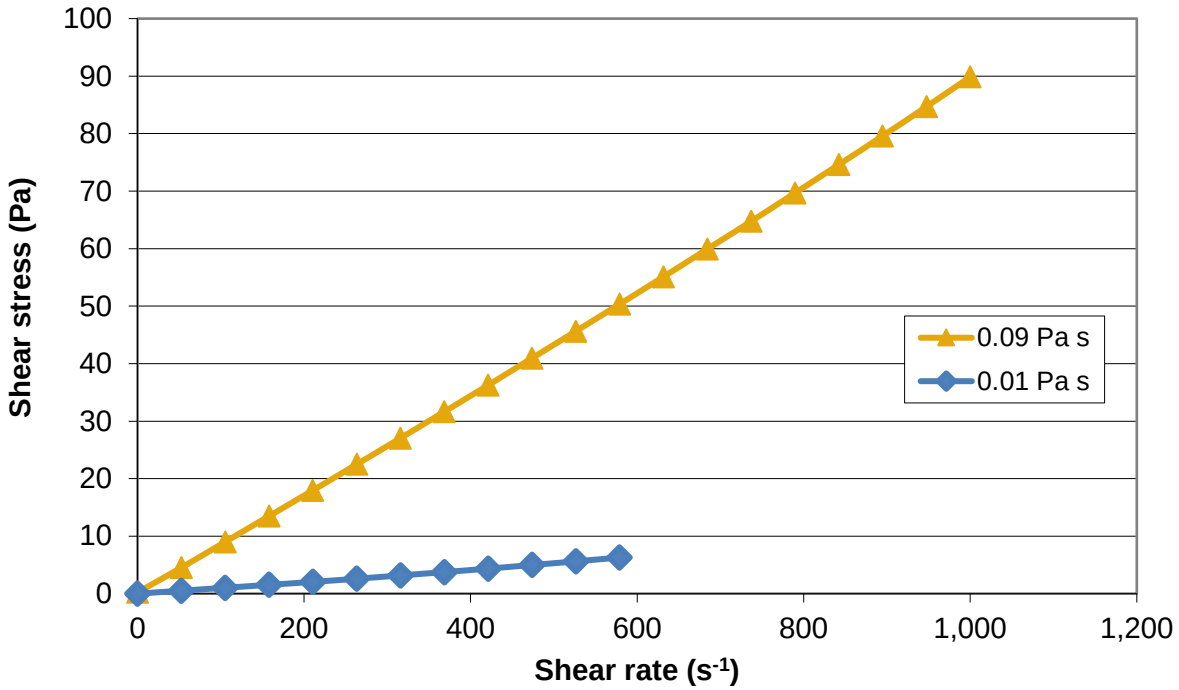

Figure 4. Flow curves for 1% wt. Aerosil® 200V-in-glycerol dispersions

The effect of powder concentration studied in water showed that as the concentration is increased, the flow behaviour of the pre-dispersions become non-Newtonian. The pre-dispersion of 15% wt. Aerosil® 200V-in-water, which was sonicated for 10 min at 50% amplitude, showed pseudoplastic behaviour as also shown in Figure 5:

$$\tau = 0.033\ \dot{\gamma}^{0.81} \qquad r^2 = 0.9998 \qquad [8]$$

Chen et al (2005) who studied the rheology of Aerosil® 200 (non-densified silica) in water also reported Newtonian behaviour up to a particle concentration of about 8% wt., and pseudoplastic behaviour at 12% wt. After one pass through the Microfluidizer, the dispersion became Newtonian with a viscosity of 0.006 Pa s and at the end of the second pass, the viscosity further decreased to 0.004 Pa s. Fumed silica dispersions tend to form 3-dimensional structures and as the particle concentration is increased the resulting gel-like structure becomes stronger

as was reported for Aerosil® 200-in-water by Chen et al (2005) and Aerosil® R816-in-water by Padron et al (2008). The evolution of the rheology for 15% wt. Aerosil® 200V dispersion during the course of processing with the Microfluidizer shown in Figure 5 would be due to the high specific power input from this device breaking the gel-like structure.

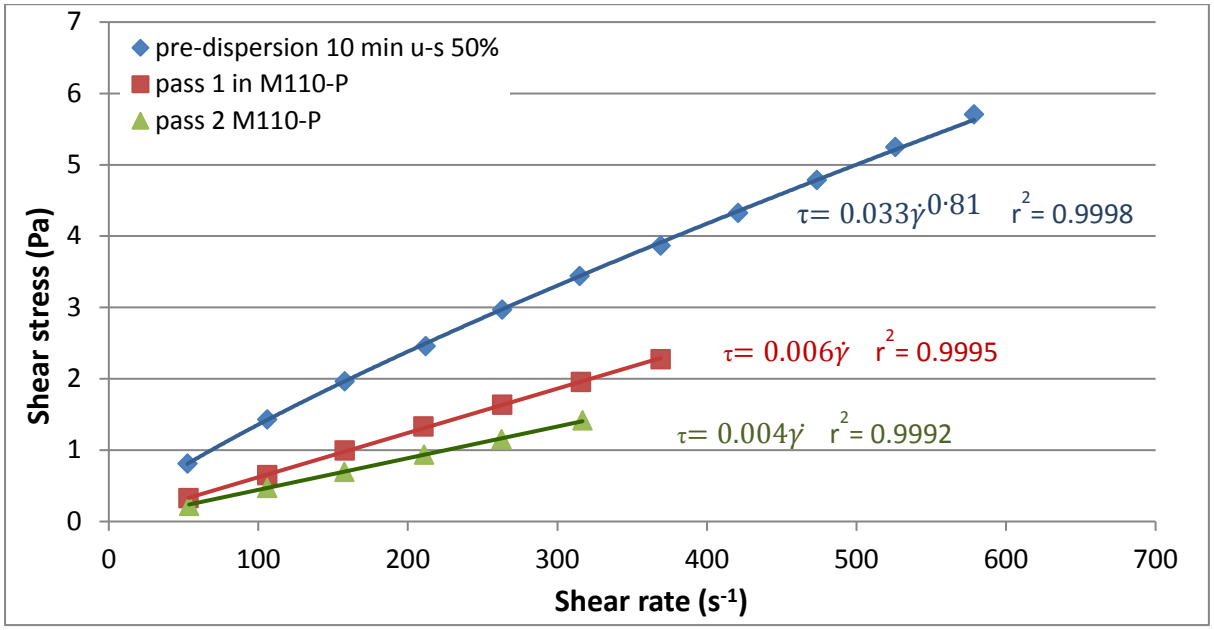

Figure 5. Flow curves for the 15% wt. Aerosil® 200V in water pre-dispersion and those during processing using the Microfluidizer M110-P

The pre-dispersion at 17% wt. was also pseudoplastic:

$$\tau = 0.051\ \dot{\gamma}^{0.79} \qquad r^2 = 0.9992 \qquad [9]$$

A comparison of the flow curves for 15% and 17% wt. pre-dispersions can be seen in Figure 6. Processing the 17% wt. pre-dispersion using the Microfluidizer also resulted in a Newtonian final dispersion with a viscosity of 0.005 Pa s as was observed with the 15% dispersion.

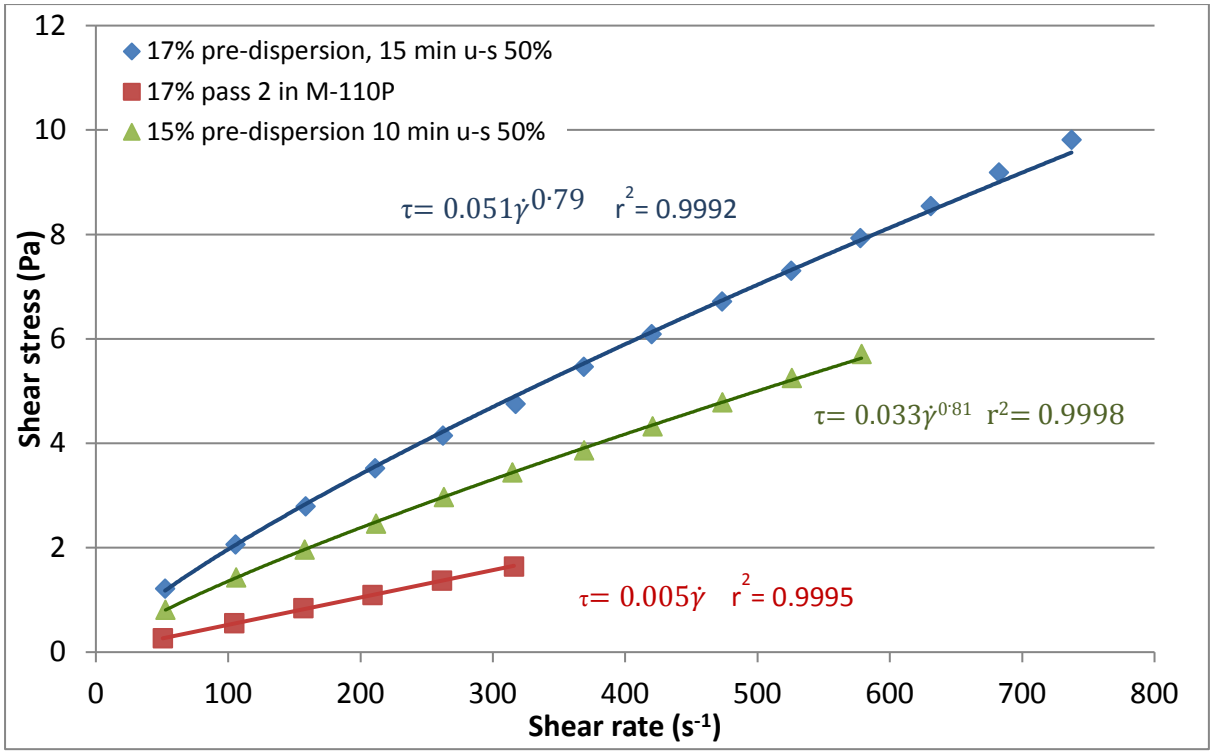

Figure 6. Comparison of the flow curves of 15 and 17% wt. pre-dispersions and the final dispersion at 17% wt. Aerosil® 200V in water

These viscosity values correspond to Reynolds number values of around 2.6×10^4 and 2.3×10^4 for 15% and for 17% particle concentrations respectively, hence the flow conditions are not very different to those at 1% concentration.

3.2 Mechanism of breakup of nanoparticle clusters using the Microfluidizer

Overall, the breakup process was fast when using the Microfluidizer and the process could be completed in one pass over a range of conditions. This would be expected considering the high level of specific power input when using this device and the volume of the dispersion. For the operating conditions that required more than one pass, the evolution of the Particle Size Distribution (PSD) indicated that breakup occurs through erosion as shown in Figure 7.

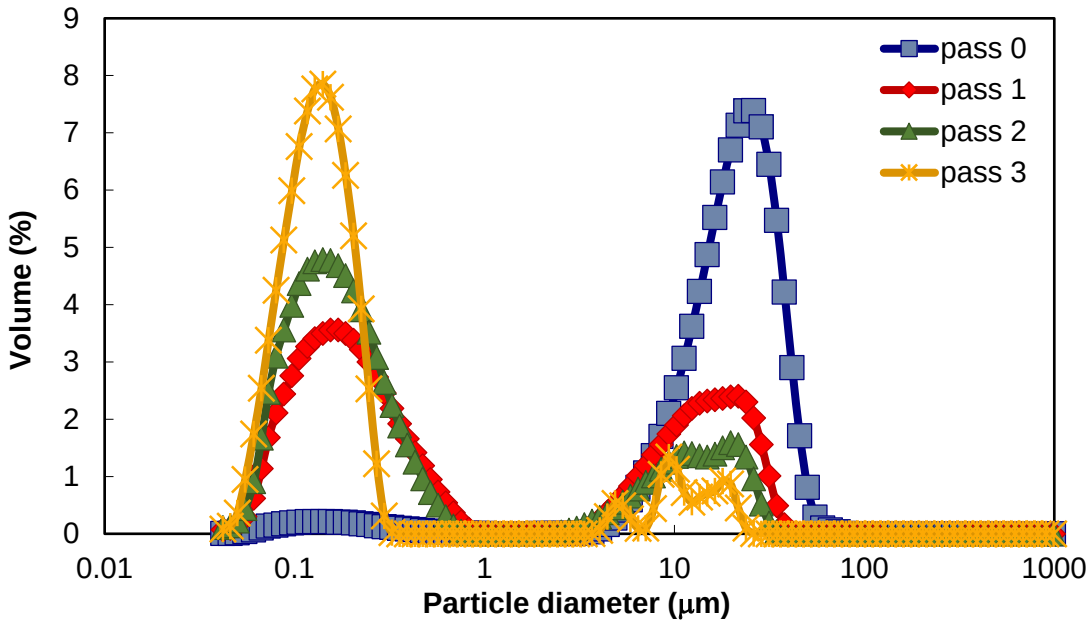

Figure 7. Evolution of PSD for 1% Aerosil® 200V-in-glycerol solution of 0.01 Pa s at an operating pressure of 35 MPa

Erosion was found to be the dominant mechanism of breakup with Aerosil® 200V-in-water in our previous studies with different types of in-line rotor-stators over a range of operating conditions (Padron et al, 2008; Özcan-Taşkin et al, 2009 and 2016). This also appears to be the case using the Microfluidizer when the continuous phase is a glycerol solution. These results obtained in the high specific power input range achieved using the Microfluidizer confirm that the break up mechanism is primarily determined by material properties, i.e. the solid-liquid pair.

Due to the bi-modal feature of the PSDs, data were analysed separately for fines, i.e. submicron material, and the evolution in time of the Sauter mean diameter or volume fraction of fines, rather than the whole dispersion, were monitored during the course of processing.

3.3 Combined effect of particle concentration and power input on the kinetics of breakup

The effect of particle concentration was investigated with only water based dispersions. At low particle concentrations of 1 and 5% wt., one pass was sufficient to break up all the agglomerates in a size range of 10's of microns into submicron aggregates (Figure 8.a).

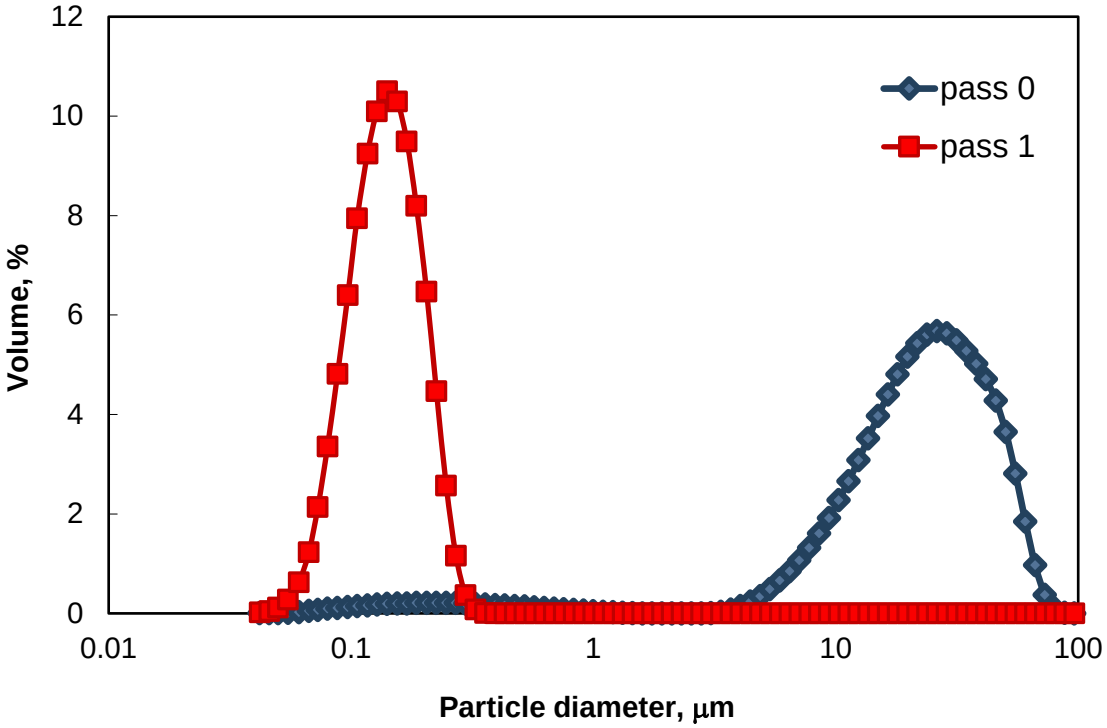

(a)

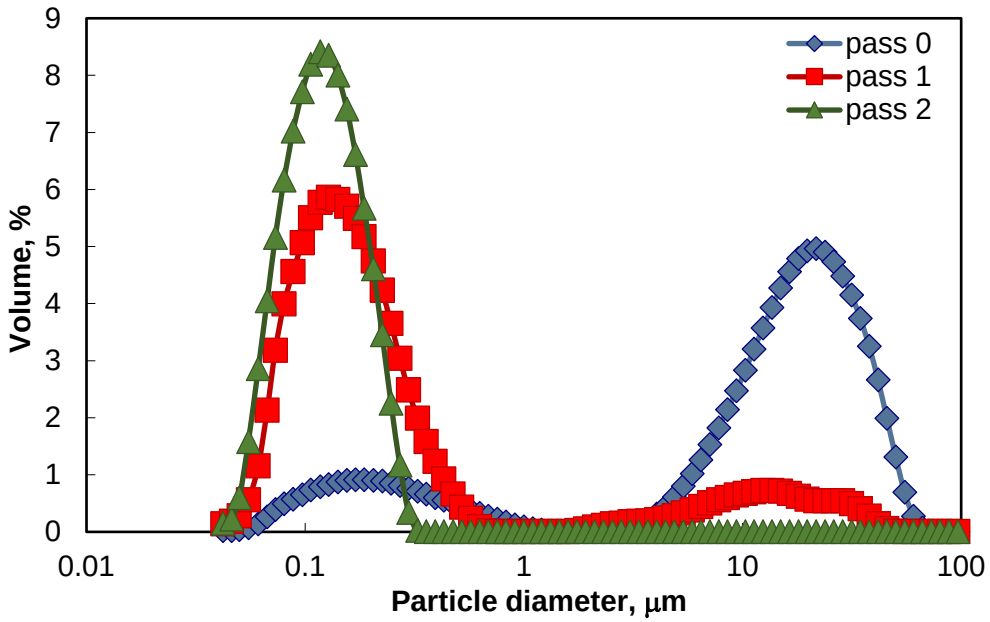

(b)

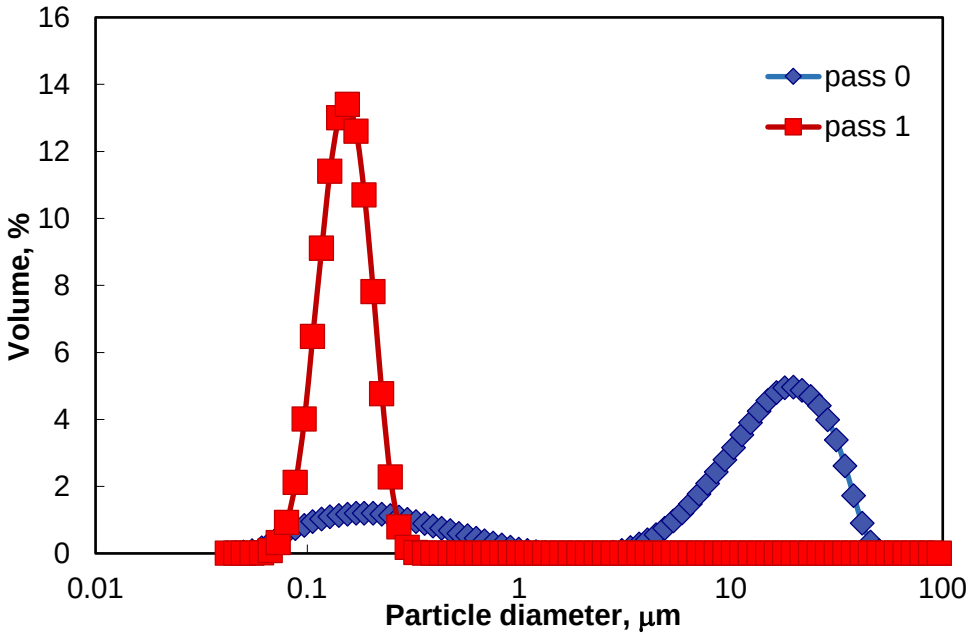

(c)

Figure 8. Combined effect of particle concentration and power input on breakup kinetics using the Microfluidizer: (a) 5% wt. Aerosil® 200V-in-water at 35 MPa;

(b) 10 % wt. Aerosil® 200V-in-water at 35 MPa;

(c) 10% wt. Aerosil® 200V-in-water at 69 MPa.

Increasing the concentration to 10% wt. and above required more passes to achieve complete break up, i.e. to obtain a dispersion that contains only sub-micron material as shown in Figure 8b. Data presented in Figure 8b also point towards an erosive type breakup with Aerosil® 200V-in-water in line with the result shown for the glycerol based dispersion in Figure 7. Increasing the operating pressure and hence the power input resulted in a reduced number passes the complete the process (Figure 8.c).

The combined effect of power input and particle concentration is shown in Table 2 with the percentage of fines achieved under different conditions. The pre-dispersion already contains a certain percentage of fines due to the pre-processing with the ultrasonicator, albeit

briefly, as explained above. For all cases considered, the percentage of fines after the first pass is greater than 85%, and 100% fines, i.e. complete deagglomeration, could be achieved.

Table 2. Summary of findings on the performance of the Microfluidizer with increasing solids concentration: percentage of fines achieved every pass at different operating pressures

	35MPa				69 MPa			103 MPa	
concentration	1%	5%	10%	15%	10%	15%	17%	15%	17%
n. of passes									
0	20	4	17	25	24	16	12	21	31
1	100	100	86	91	100	95	96	100	100
2			100	100		100	100		

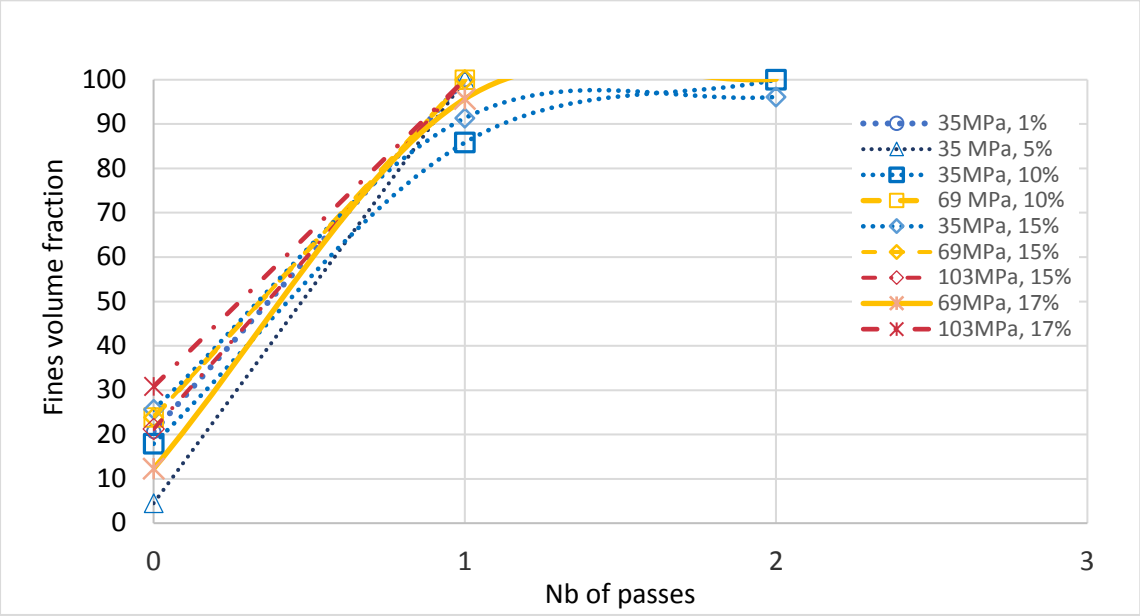

Figure 9. Effect of particle concentration and operating pressure (power input) on the kinetics of breakup

In Figure 9, data analysed in terms of fines volume fraction are shown and Table 3 summarises the combined effect of particle concentration and power input: as the particle concentration is increased, either a higher number of passes is required or the power input needs

to be increased for a given number of passes. It can be noted that overall the process is fast and only a few passes through the device are required to produce a fine dispersion.

Table 3. Summary of results on the performance of the Microfluidizer with increasing particle concentration: number of passes necessary to achieve 100% break-up to fines

		Pressure drop, MPa		
		35	69	103
Concentration, % wt	1	1	-	-
	5	1	-	-
	10	2	1	-
	15	2	2	1
	17	2+	2	1

3.4 Combined effect of continuous phase viscosity and power input on breakup kinetics

The effect of continuous phase viscosity was studied using glycerol solutions at a particle concentration of 1% wt. Whilst one pass was sufficient to completely deagglomerate 1 and even 5% wt. Aerosil® 200V in water at 35 MPa (Figure 8.a), a ten fold increase in the continuous phase viscosity to 0.01 Pa s tripled the required number of passes (Figure 7). By increasing the power input to 103 MPa, the number of passes required to achieve complete deagglomeration could be reduced as a comparison of Figures 7 and 10 shows.

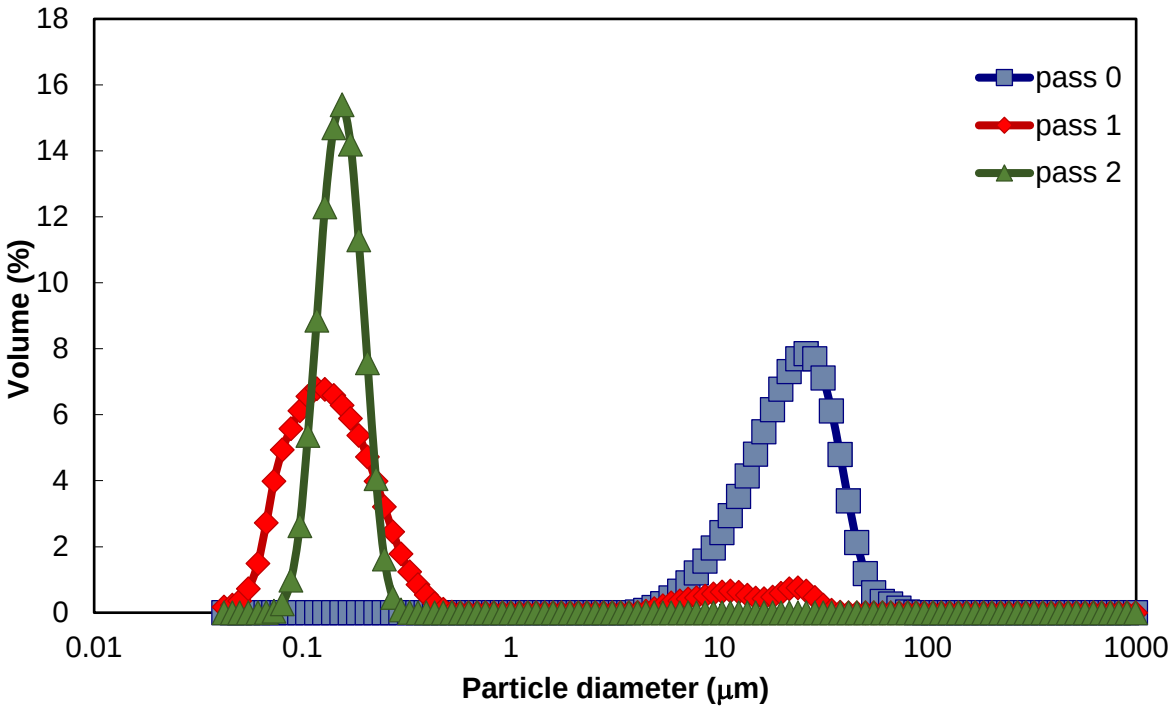

Figure 10. Evolution of PSD during the break up of 1% wt. Aerosil® 200V in 0.01 Pa s glycerol using the Microfluidizer operated at 103 MPa

This can also be seen for the dispersion in 0.09 Pa s glycerol: an increase in power input reduces the number of passes required to achieve complete breakup (Figures 11a and 11b).

Table 4 summarises the percentage of fines obtained at each pass through the Microfluidizer for varying continuous phase viscosities and operating pressures. The pre-dispersion already contains a certain percentage of fines due to pre-processing with the ultrasonicator. After one pass through the Microfluidizer more than 60% of fines is achieved for the conditions covered.

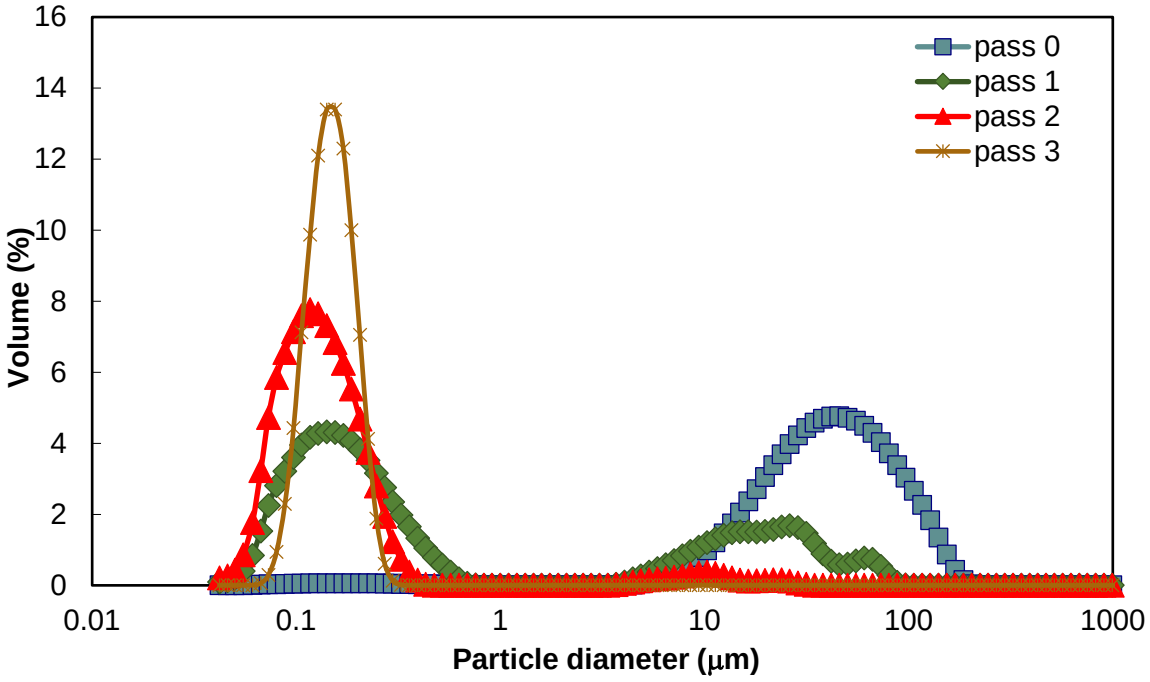

(a)

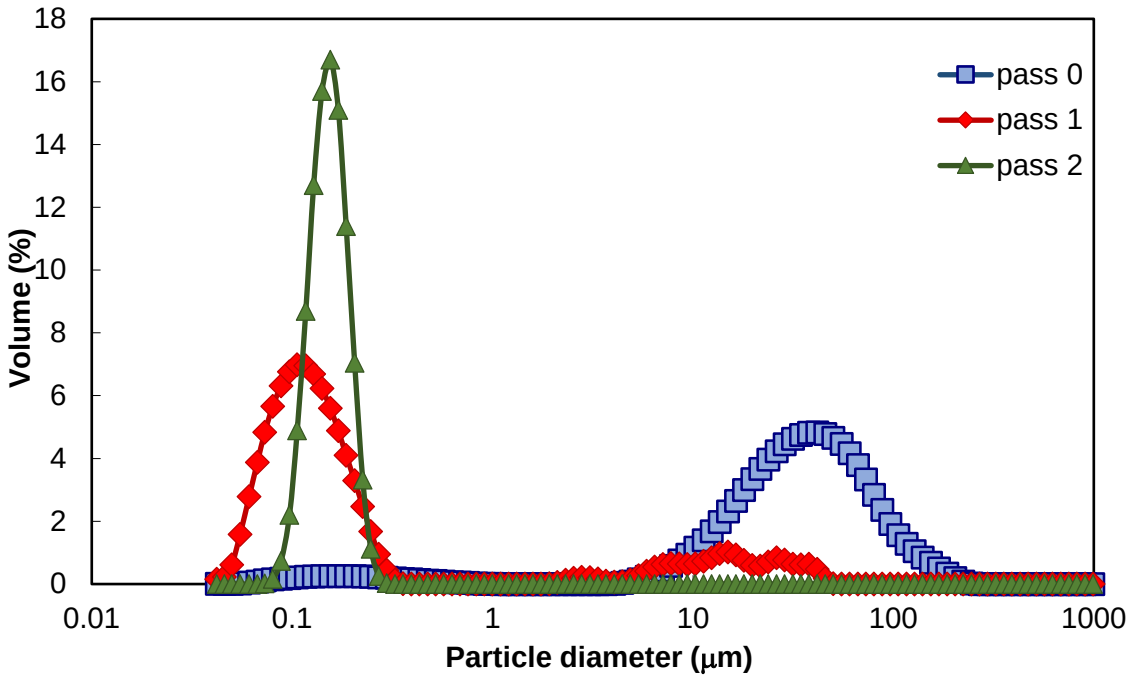

(b)

Figure 11. Effect of power input: (a) 69 MPa and (b) 103 MPa on the break up process for 1% wt. Aerosil® 200V in glycerol dispersion at 0.09 Pa s.

Table 4. Summary of findings on the performance of the Microfluidizer for increasing viscosities: percentage of fines achieved every pass at different operating pressures

	35 MPa		69 MPa		103 MPa	
Viscosity (Pa s) n. of passes	0.001	0.010	0.010	0.090	0.010	0.090
0	20	4	4	1	0	5
1	100	61	87	68	90	83
2		76	100	96	100	100
3		88		100		

A comparison of data analysed in terms of fines volume fraction shows that increasing the continuous phase viscosity requires more passes to achieve complete breakup of agglomerates at a given operating pressure and the number of passes can be reduced by increasing the operating pressure (Figure 12). These are also summarized in Table 5.

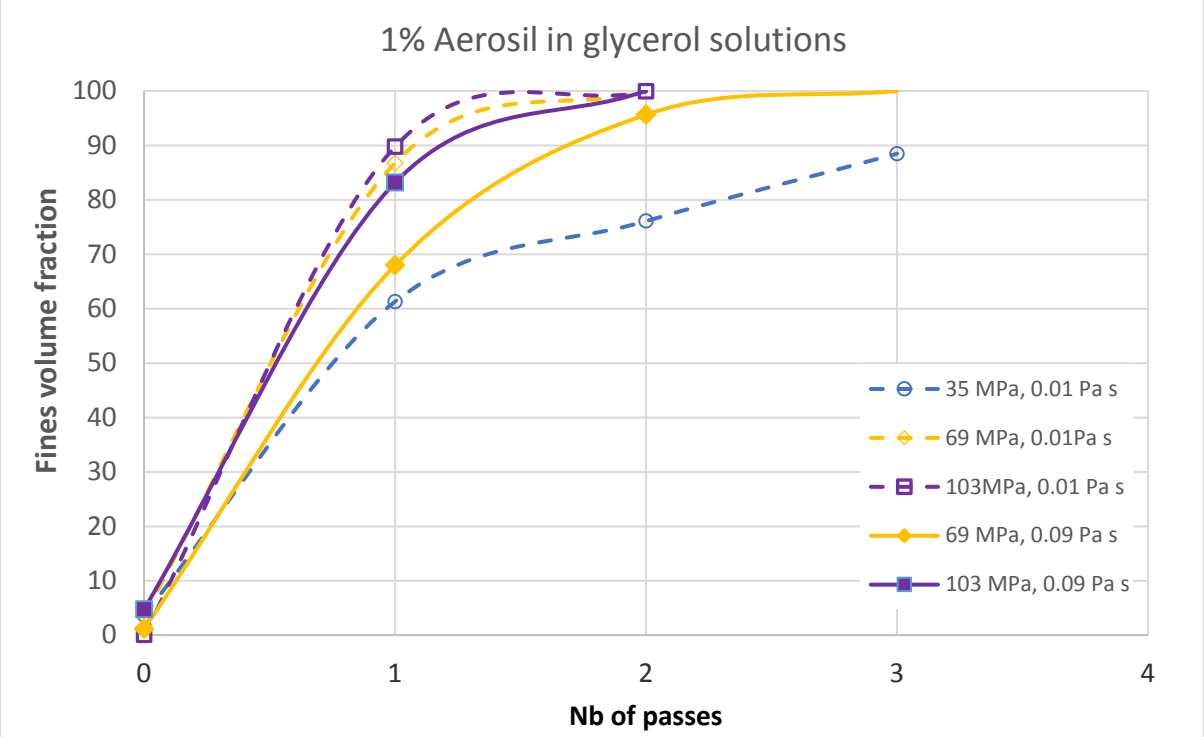

Figure 12. Effect of continuous phase viscosity and operating pressure (power input) on the kinetics of breakup

Table 5 Summary of results on the performance of the Microfluidizer for increasing continuous phase viscosity: number of passes necessary to achieve 100% break-up to fines

	Pressure drop, MPa		
Viscosity (Pa s)	35	69	103
0.001	1	-	-
0.010	3+	2	2
0.090	-	3	2

Overall, the effect of increasing viscosity was found to be more pronounced compared to the effect of increasing particle concentration in the range covered in this study. This would be due to the increase in viscosity from 0.001 to 0.090 Pa s having a more significant effect on the Reynolds number resulting in suppressed turbulence. This increase in continuous phase viscosity increases the Kolmogorov microscale (eqn 2) and in the viscous subrange the frequency of turbulence (eqn 6) decreases. Whist increasing the particle concentration also had an effect on the rheology, in particular at concentrations above 10% wt., the viscosity decreased significantly during the course of deagglomeration. It can be anticipated that the dispersion passing through the ~~auxillary~~auxiliary chamber prior to reaching the interaction chamber, was already of a lower viscosity and hence the effect on the breakup process was reduced.

3.5 Dispersion fineness- the smallest attainable size

The Sauter mean diameter of the fines has been found to be around 150 nm as shown Figure 13 regardless of the operating condition, dispersed phase concentration or continuous phase viscosity. As this is much larger than the primary particle size given for Aerosil® 200V it can be concluded that the smallest attainable size is that of aggregates rather than the primary

particles. This is due to the manufacturing method employed, flame pyrolysis, which takes place at very high temperatures. Collision, coalescence and partial fusion of the primary particles at high temperatures result in the formation of aggregates held together via strong ≡Si-O-Si≡ bridges (Gun'ko et al, 1998).

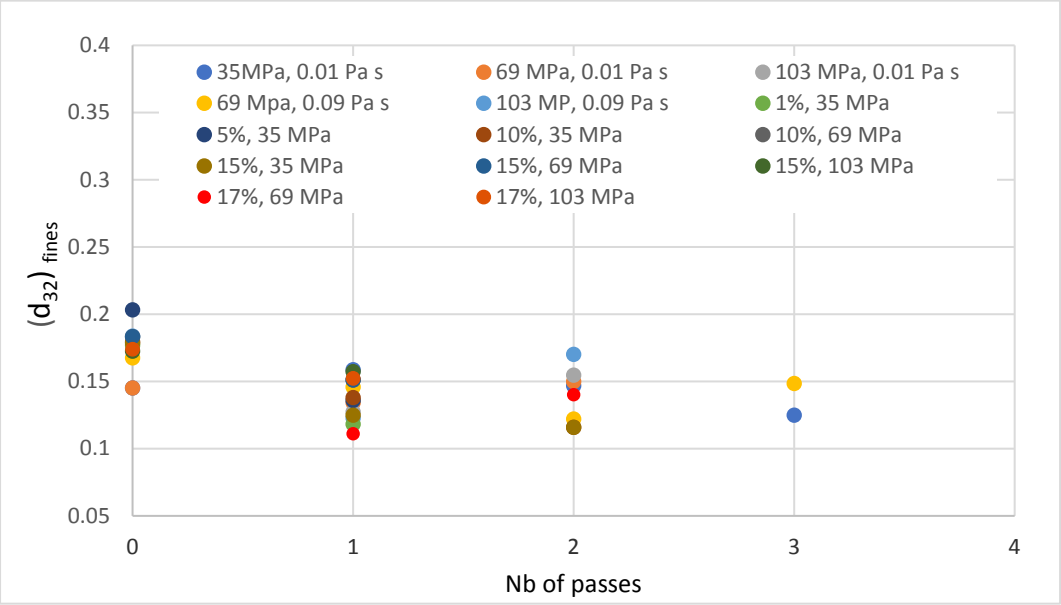

Figure13. Sauter mean diameter of fines obtained using the Microfluidizer M110-P

3.6 Comparative equipment performance

The comparative performance of the specific microfluidic device used was evaluated in terms of the mechanisms and kinetics of breakup as well as dispersion fineness. The dominant mechanism of breakup, erosion, was also the breakup mechanism reported for other process devices such as in-line (Padron et al, 2008; Özcan-Taşkin et al, 2016) and batch rotor-stators (Xie et al, 2008; Kamaly et al, 2017), a saw-tooth impeller or a valve homogenizer (Xie et al, 2008) for this particle-liquid pair.

Figure 14 compares the Sauter mean diameters of fines obtained with the Microfluidizer and in-line rotor-stators, which is around 150 nm irrespective of the device or operating condition. Based on these results, it can be concluded that both the mechanism of break up and

the mean diameter of fines are independent of operating conditions even at such high specific power input values that could be reached using the Microfluidizer.

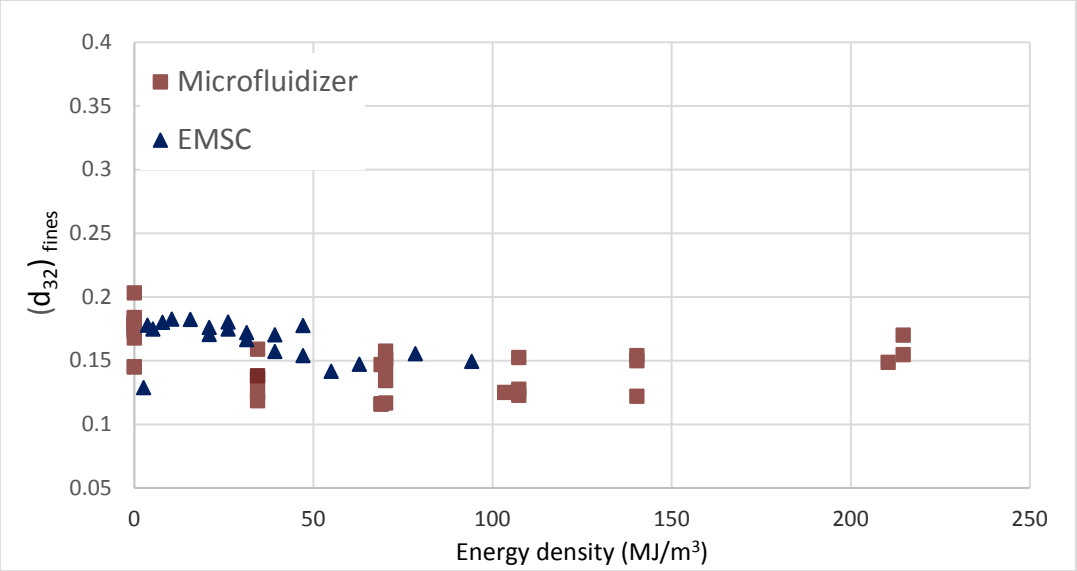

Figure 14. Comparison of the Sauter mean diameter of fines obtained using the Microfluidizer M110-P and in-line rotor-stators

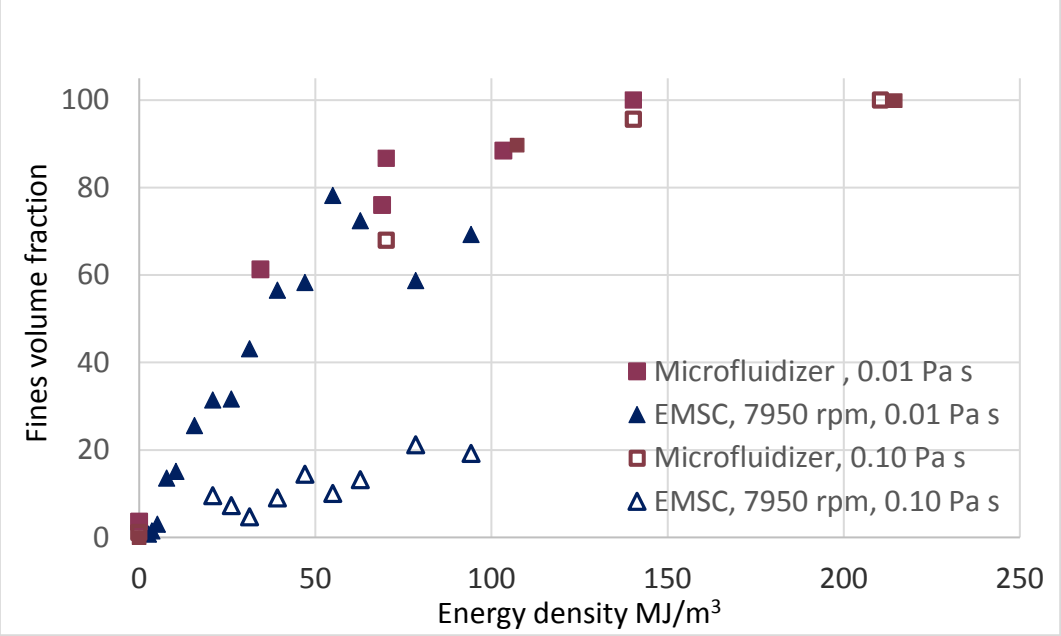

Figure 15. Breakup kinetics of Microfluidizer compared to an in-line rotor-stator

The kinetics of breakup can be considered to be similar for the two devices when compared on the basis of energy density at the lower viscosity of 0.01 Pa s. Increasing the viscosity to 0.09 Pa s had a more drastic effect on the breakup kinetics with the inline rotor-stator and the fines generation rate was much higher with the Microfluidizer as can be seen in Figure 15. Increasing the continuous phase viscosity would also result in an increase in the Kolmogorov length scale and a decrease in the frequency of turbulence; in addition the specific power input is much lower with this device compared to the Microfluidizer as highlighted in Section 3.1. Whilst the two devices would not be considered as an alternative to one another as much larger volumes (of the order of 100 litres) would typically be processed with the in-line rotor-stator compared to this specific bench top Microfluidizer, the differences in the dispersion volume are taken into account in the volumetric energy input to evaluate the kinetics of breakup.

4. CONCLUSIONS

A bench-top commercial design microfluidic device, Microfluidizer M110-P, was used to assess its performance in deagglomerating clusters of nanoscale silica particles. The effects of increasing particle concentration and continuous phase viscosity on the mechanisms and kinetics of breakup as well as the dispersion fineness were studied in conjunction with that of the power input.

The specific power input of the device was determined to be in the range of 7.8×10^{3} to 1.5×10^{5} kW m^{-3} for operating pressures of 5 to 15 kpsi (or 35 to 103 MPa). This is significantly higher than the range typically covered with other power intensive devices used in industry such as batch or in-line rotor-stators.

From this investigation, it could be concluded that the Microfluidizer can be used to achieve complete deagglomeration of Aerosil® 200V silica particles at concentrations up to 17% wt. in water or continuous phase viscosities up to 0.09 Pa s at 1% wt. It is worth noting

that the pre-dispersion can require pre-treatment to reduce the agglomerates size to avoid blockage of channels. In addition, the product can reach very high temperatures if appropriate measures are not taken.

A single pass was sufficient to achieve breakup at 1 and 5% wt. Aerosil® 200V-in-water at the lowest pressure value of 35 MPa. Increasing the particle concentration or continuous phase viscosity slowed down breakup kinetics and either a higher number of passes or a higher power input (for the same number of passes) was required to obtain a dispersion which has a size distribution in the submicron range. The effect was more pronounced for increased continuous phase viscosities covered in this study as this would both increase the Kolmogorov lengthscale and decrease the frequency of turbulence in the viscous subrange. At particle concentrations above 10% wt., the pre-dispersion showed pseudoplastic behaviour which subsequently became Newtonian and of a lower viscosity, ~0.004- 0.006 Pa s at the end of the deagglomeration process. Whilst glycerol based 1% wt. dispersions were Newtonian, increasing the continuous phase viscosity by about two orders of magnitude had a marked effect on the Reynolds number which decreased from 3.8×10^4 for 1% wt. Aerosil® 200V-in-water to about 8.8×10^2 in 0.09 Pa s dispersion. This would have had a more significant effect in the flow field suppressing turbulence and hence a lower volume fraction of fines under given operating conditions as the viscosity is increased. It is worth bearing in mind that the use of a different continuous phase may also affect particle-liquid affinity and results with a different continuous phase may be different in the same viscosity range.

The predominant break up mechanism was found to be erosion. The dispersion fineness was defined by the aggregate size rather than that of primary particles and the Sauter mean diameter of the aggregates was around 150 nm. These findings are in agreement with those reported using other process devices, which operate in a comparatively lower specific power

input range. Therefore, it can be concluded that the mechanism of breakup and dispersion fineness are primarily determined by material properties rather than operating conditions.

The breakup kinetics evaluated on the basis of specific energy input was comparable to that of an in-line rotor-stator at a viscosity of 0.01 Pa s but increasing the viscosity further to 0.09 Pa s, showed a higher fines generation rate with the Microfluidizer. Whilst these two devices would not be considered as alternatives for an industrial process as the Microfluidizer used was a bench top model that would typically be used for product formulation stage whereas the in-line rotor-stator can handle much larger volumes, it is still useful to assess their comparative performance. Larger units exist which operate at much higher flow rates and future work may make use of these devices as well.

Acknowledgements The authors gratefully acknowledge the financial and technical contributions of the industrial members of the DOMINO consortium as well as the discussions held with the consultants, Prof Jerzy Baldyga of Warsaw University of Technology and Dr Art Etchells.

NOMENCLATURE

d	Interaction chamber channel diameter	(m)
d_{32}	Sauter mean diameter (area-weighted average particle size)	(μm)
E_v	Energy density	(MJ m^{-3})
l	Macroscale of turbulence	(m)
L_i	Agglomerate size	(m)
m	Mass of dispersion	(kg)
P	Power input	(W)
p_i	Operating pressure	(Pa)

Q_i	Impulse flow rate	($m^3\ s^{-1}$)
Re	Reynolds number ($4\ Q_i\ \rho/\mu\pi d$)	(-)
t_i	Time of impulse	(s)
V_i	Volume of impulse	(m^3)

Greek

ε	Local energy dissipation rate per unit mass of liquid	($m^2\ s^{-3}$)
$\dot{\gamma}$	Shear or extensional rate	(s^{-1})
λ_k	Kolmogorov microscale	(m)
μ	Shear or extensional viscosity	(Pa s)
ρ	Density	($kg\ m^{-3}$)
τ	Shear or extensional stress	(Pa)
ν	Kinematic viscosity	($m^2\ s^{-1}$)

REFERENCES

Bai, L.; McClements, D. J. (2016) Development of microfluidization methods for efficient production of concentrated nanoemulsions: Comparison of single- and dual-channel microfluidizers. Journal of Colloid and Interface Science, Vol. 466, p: 206-212 doi.org/10.1016/j.jcis.2015.12.039

Bałdyga, J., Bourne, J. R. (1994) “Drop breakup in the viscous subrange: a source of possible confusion” Chem. Eng. Sci., 49, p:1077- 1078.

Baldyga, J.; Orciuch, W.; Makowski, L.; Malik, K.; Özcan-Taşkin, G.; Eagles, W.; Padron, G. (2008) “Dispersion of nanoparticles in a rotor-stator mixer" Ind. Eng. Chem. Res., 47 (10), 3652 -3663. DOI 10.1021/ie070899u.

Chen, S.; Øye, G.; Sjöblom, J. (2005) Rheological properties of aqueous silica particle suspensions. J. Dispersion Sci. Technol., 26, 495.

Choi, H.; Laleye, L.; Amantea, G.F.; Simard, R.E. (1997) Release of aminopeptidase from Lactobacillus casei sp. casei by cell disruption in a Microfluidizer. Biotechnology Techniques, Vol 11, No 7, July 1997, pp. 451–453

Chomistek, K. J.; Panagiotou, T. (2009) Large scale nanomaterial production using microfluidizer high shear processing. Materials Research Society Symposia Proceedings Vol.1209, p:85 -P03-01.

Gun'ko, V.M.; Zarko, V.I.; Leboda, R.; Voronin, E.F.; Chibowski, E.; Pakhlov, E.M. (1998) Influence of modification of fine silica by organosilicon compounds on particle-particle interaction in aqueous suspensions. Colloids Surf. A, 132 (2–3): 241–249.

Kamaly, S.W.; Tarleton, A.; Özcan-Taşkın, N. G. (2017) Dispersion of clusters of nanoscale silica particles using batch rotor-stators. Advanced Powder Technology, Vol. 28, Issue 9, p: 2357- 2365 //doi.org/10.1016/j.apt.2017.06.017

Kühler, S.; Schneider C.; Lerch, D.; Sobisch T. (2006) Process optimisation for making stable emulsions using accelerated dispersion analysis by multisample analytical centrifugation. LabPlus International 20/4, p: 14- 17.

Lajunen, T.; Hisazumi K.; Kanazawa T.; Okada H.; Seta Y.; Yliperttula M.; Urtti A.; Takashima, Y. (2014) Topical drug delivery to retinal pigment epithelium with microfluidizer produced small liposomes. European Journal of Pharmaceutical Sciences 62 (2014) 23–32. doi.org/10.1016/j.ejps.2014.04.018

Lee, L.; Norton, I.T. (2013) Comparing droplet breakup for a high-pressure valve homogeniser and a Microfluidizer for the potential production of food-grade nanoemulsions. Journal of Food Engineering 114; p:158–163, doi.org/10.1016/j.jfoodeng.2012.08.009

Özcan-Taşkin, N. G.; Padron, G. and Voelkel, A. (2009) "Effect of particle type on the mechanisms of breakup of nanoscale particle clusters" Chem. Eng. Res. Des., 87, No.4, p: 468-473. doi:10.1016/j.cherd.2008.12.012

Özcan-Taşkın, N. G., Kubicki, D., & Padron, G. A. (2011) Power and flow characteristics of three rotor-stator heads. The Canadian Journal of Chemical Engineering, 89(5), 1005–1017. doi:10.1002/cjce.20553

Özcan-Taşkin, N. G.; Padron, G. A.; Kubicki, D. (2016) Comparative performance of in-line rotor-stators for deagglomeration processes. Chem. Eng. Sci., 156 p:186–196. doi.org/10.1016/j.ces.2016.09.023

Padron, G. A. (2001) Measurement and comparison of power draw in rotor-stator mixer. MSc thesis, University of Maryland, College Park, MD, USA.

Padron, G. A.; Eagles, W.P.; Őzcan-Taşkin, G. N.; McLeod, G. and Xie, L. (2008) Effect of particle properties on the breakup of nanoparticle clusters using an in-line rotor-stator. Jrnl of Disp. Sci. and Tech., Vol 29, Issue 4, p:580-586. DOI 10.1080/01932690701729327

Padron, G. A.; Őzcan-Taşkin, N. G. (2017) Particle de-agglomeration with an in-line rotor-stator mixer at different solids loadings and viscosities. ISMIP9 Oral presentation, 25- 28 June, 2017; Birmingham UK.

Panagiotou, T.; Mesite, S.V.; Fisher, R.J. (2009) Production of norfloxacin nanosuspensions using microfluidics reaction technology through solvent/ antisolvent crystallization, Ind. Eng. Chem. Res. 48 1761–1771. doi: 10.1021/ie800955t

Persson K.H.; Blute I.A.; Mira, I.C.; Gustafson, J. (2014) Creation of well-defined particle stabilized oil-in-water nanoemulsions Colloids and Surfaces A: Physicochem. Eng. Aspects, (459), 48- 57, doi.org/10.1016/j.colsurfa.2014.06.034

Sauter C.; Schuchmann H. P. (2007) High pressure for dispersing and de-agglomerating nanoparticles in aqueous solutions. Chemical Engineering and Technology, Vol. 30, No.10; p: 1401- 1405.

Stupak, R.; Makauskas, N.; Radzevicˇius, K.; Valancˇius, Z. (2015) Optimization of Intracellular Product Release from Neisseria denitrificans Using Microfluidizer. Preparative Biochemistry & Biotechnology, 45:667–683. doi: 10.1080/10826068.2014.940539

Wengeler, R.; Teleki, A.; Vetter, M.; Pratsinis, S.E.; Nirschl, H. (2006) High-pressure liquid dispersion and fragmentation of flame-made silica agglomerates. Langmuir 2006, 22, 4928-4935.

Xie, L.; Rielly, C.D.; Eagles, W.P.; Őzcan-Taşkin, N.G. (2007) Dispersion of nanoparticle clusters using mixed flow and high shear impellers in stirred tanks. Chem. Eng. Research and Design, 85 (A5), p: 676-684. DOI: 10.1205/cherd06195

Xie, L.; Rielly, C.D.; and Őzcan-Taşkin, N.G. (2008) Break-up of nanoparticle agglomerates by hydrodynamically limited processes. Journal of Dispersion Science and Technology, 29, 4, p: 573- 579. **DOI:**10.1080/01932690701729211

Yurdakul, H.; Göncü, Y.; Durukan, O.; Akay, A.; Seyhan. T.; Ay N.; Turan S. (2012) Nanoscopic characterization of two-dimensional (2D) boron nitride nanosheets (BNNSs) produced by microfluidization. Ceramics International, Vol.38, Issue 3, p: 2187- 2193. doi.org/10.1016/j.ceramint.2011.10.064